

LIBRARY  
TECHNICAL REPORT SECTION  
NAVAL POSTGRADUATE SCHOOL  
MONTEREY, CALIFORNIA 93940

131282  
JR  
✓ Technical Report No. 20

SACLANT ASW  
RESEARCH CENTER

FREQUENCY DEVIATION INDICATOR

by

H.A.J. RYNJA

20 November 1963

VIALE SAN BARTOLOMEO, 32  
LA SPEZIA, ITALY

AD0808758



TECHNICAL REPORT 20

SACLANT ASW RESEARCH CENTER

Viale San Bartolomeo 92

La Spezia, Italy

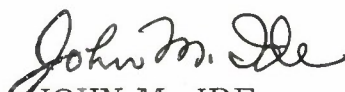
FREQUENCY DEVIATION INDICATOR

By

H. A. J. Rynja

20 November 1963

APPROVED FOR DISTRIBUTION

  
JOHN M. IDE

Director





## FREQUENCY DEVIATION INDICATOR

By

H. A. J. Rynja

### Summary

A new type of discriminator has been developed to measure the frequency variation of electrical signals; it has the special feature to indicate without any delay the difference between the signal frequency and some fixed reference frequency.

The discriminator consists of two different parallel, frequency sensitive, networks, the outputs of which are always either in phase or in phase opposition but have different amplitudes. On a CRT screen these two voltages produce a line; the length of the line gives the amplitude and its direction gives the frequency of the original signal. By a proper choice of some circuit parameters, the indication can be made linear with the frequency within a relatively large frequency band. Between the limits of noise and overload of the amplifiers, the signal amplitude has no influence on the indicated angle.

The same networks can be used to construct a simple discriminator that produces a DC voltage proportional to the frequency deviation as is done by FM demodulator circuits. Among the many applications of this discriminator this report describes the registration of the changes in the earth's magnetic field with the use of a Rubidium Vapour Magnetometer and the recording of the variations in the sound velocity in sea water using a Daystrom Sound Velocity Meter.



## INTRODUCTION

The indication of the frequency variations of an electrical signal requires a frequency sensitive instrument. There are many circuits that give a response on frequency variations, called "discriminators," well known for demodulation of FM signals. Most of the discriminators are composed of resonant circuits or delay lines followed by a rectifier. Due to the delay line, or to the DC filter following the rectifier, all these circuits inhibit a certain time constant. Furthermore, the amplitude of the original signal sometimes influences, more or less, the output voltage so that an amplitude limiter is needed to reduce the variations in signal voltage. However, limiters are only effective in a restricted frequency band; they have a certain time constant **also, and they never reduce the** signal variations to zero. Therefore, when the frequency of short signal pulses or amplitude modulated signals has to be measured, most of the known discriminator circuits are unable to give a clear and precise indication.

The instrument described gives a representation of the frequency deviation  $\Delta f_o$  from a certain frequency  $f_o$  of a sinusoidal electric signal. The indication is independent of the amplitude of the signal and is without any time delay. However, it is well known that the frequency of an amplitude modulated signal cannot be given by only one number; instead, it is represented by a certain frequency band depending on the waveform of the modulation. It is clear that this uncertainty in the numerical value of the frequency will be recorded also.

The indication appears on an oscilloscope screen as the angle of inclination  $\phi$  of a straight line. It can be proved that a proper choice of various circuit parameters results in a symmetric frequency deviation scale.

[REDACTED]

This last fact is important when the frequency deviations are of the same magnitude as the mean frequency. Many frequency selective networks give a response that is symmetrical on a logarithmic frequency scale, so that the same output in absolute value will be found for any pair of frequencies  $pf_0$  and  $\frac{f_0}{p}$ . However, the linear symmetry of the discriminator described here means that the same angles  $+\phi$  and  $-\phi$  are indicating the frequencies of  $f_0 + \Delta f_0$  and  $f_0 - \Delta f_0$ .

If a time-record of the frequency deviations is desired, a phase sensitive detector can be added to the circuit, giving a DC voltage more or less proportional to the frequency deviation  $\Delta f_0$ . This can be recorded on any DC paper recorder. In this case, a limiter is needed also, and the instrument offers no advantage over other conventional discriminators which have a certain time constant. However, it can be said, that the circuit is very simple, and a relatively large frequency band (0 to  $2f_0$  and even higher) can be covered. Also, the same type of circuit can be designed for a very high sensitivity in a small bandwidth.

## PART I

### OSCILLOSCOPE DISPLAY

#### 1.1 Principle of Operation

The basic principle of the discriminator is the comparison of two signals that are produced by processing the original signal through two different frequency sensitive networks. These networks are so designed that the two signals they produce are either in phase or in phase opposition for all frequencies. These two signals are indicated respectively by  $\bar{a}$  and  $\bar{c}$ . Figure 1 gives the block diagram of the discriminator; the original signal is indicated by  $\bar{e}$ .

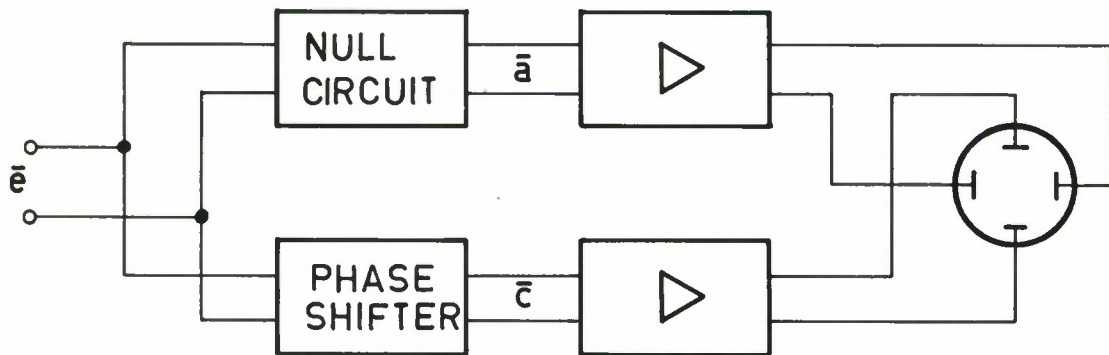


Fig. 1 Basic Block Diagram of Discriminator

The circuit that produces the signal  $\bar{a}$  is a "null circuit": at the frequency  $f_0$  the amplitude of  $\bar{a}$  goes through zero while the phase difference between  $\bar{a}$  and  $\bar{e}$  jumps from  $90^\circ$  to  $270^\circ$ . The " $\bar{c}$ -circuit" is a phase-shifter that produces a phase shift of  $90^\circ$  at the frequency  $f_0$ .

When the signals  $\bar{a}$  and  $\bar{c}$  are applied to the horizontal and vertical deflection systems of an oscilloscope, a straight line appears on the screen; the position of the line is determined by the amplitude ratio of  $\bar{a}$  and  $\bar{c}$ . In the following paragraphs, an analysis will be given for different  $\bar{a}$ - and  $\bar{c}$ -circuits in order to find the conditions for which the slope  $\phi$  of the trace on the CRT-screen is linearly proportional to the frequency deviation  $\Delta f_o$ .

## 1.2 The $\bar{a}$ -circuit

The  $\bar{a}$ -circuit is a bridge that gives complete signal extinction for one frequency; this frequency is the central frequency  $f_o$ . For the purpose of generalization of the equations, the relative frequency  $\beta$  will be introduced as

$$\beta = \frac{f}{f_o} = \frac{\omega}{\omega_o} \quad (1)$$

where  $f$  and  $\omega$  are the frequency and the angular frequency of the original signal respectively.

1.2.1 The Wien - Bridge. Figure 2 gives the circuit diagram for the Wien-Bridge. The factor  $n$  in this circuit may have any value between 0 and  $\infty$ . This fact gives the desired flexibility to the circuit in order to obtain a symmetric frequency shift indication by a proper choice of its value. (This will be discussed in Sect. 1.6). The condition to have zero output at the frequency  $f_o$  for this circuit is

$$\omega_o R_1 C_1 = 1 \quad (2)$$

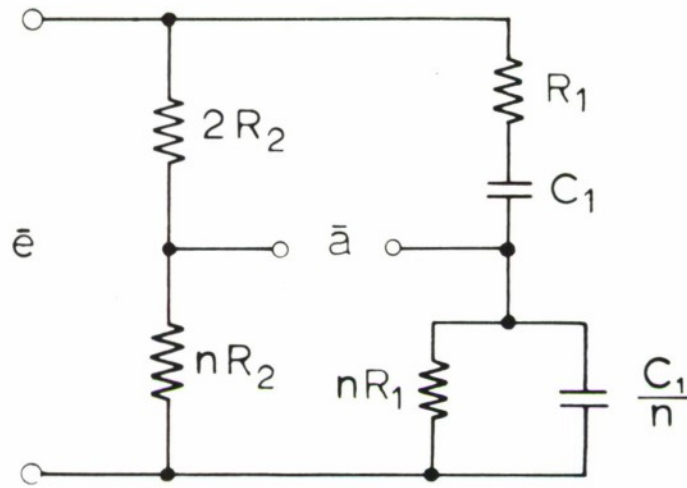


Fig. 2 Wien Bridge as Null Circuit

The value of  $R_2$  can be chosen arbitrarily.

The output voltage  $\bar{a}$  of this circuit is given by

$$\frac{\bar{a}}{\bar{e}} = \frac{n}{n+2} \cdot \frac{-1}{1 - j \frac{\beta}{\beta^2 - 1} (n+2)} \quad (3)$$

with a phase angle  $\alpha$  given by

$$\text{tg } \alpha = (n+2) \frac{\beta}{\beta^2 - 1} \quad (4)$$

The vector diagram of  $\bar{a}$  in the complex plane is given by Fig. 3.

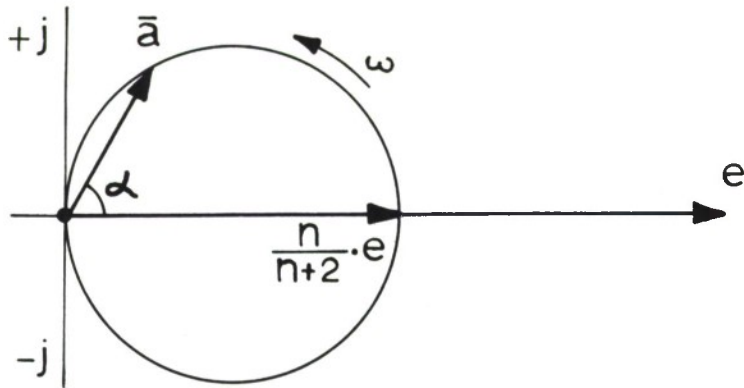
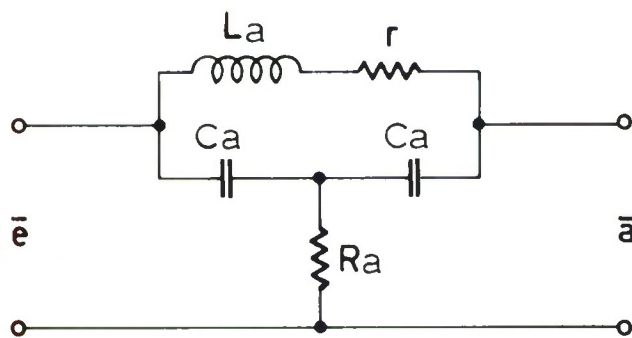


Fig. 3 Vector Diagram of the Wien Bridge

1.2.2 The Bridged-T. Figure 4 shows the circuit diagram for the Bridged-T.



The conditions for this circuit to give an output zero at the angular frequency  $\omega_o$

are

$$\omega_o^2 L_a C_a = 2 \quad (5)$$

and

$$L_a = 2r R_a C_a \quad (6)$$

Fig. 4 The Bridged-T-Null Circuit

By introducing the quality factor  $Q_a$  of the coil  $L_a$  as

$$Q_a = \frac{\omega_o L_a}{r} \quad (7)$$

and the relative frequency  $\beta$  from Eq. (1), the transfer function of the bridged-T is found to be

$$\frac{\bar{a}}{\bar{e}} = \frac{1}{1 - j \frac{\beta}{\beta^2 - 1} \cdot \frac{2}{Q_a}} \quad (8)$$



The phase angle  $\alpha$  between  $\bar{a}$  and  $\bar{e}$  is given by

$$\text{tg } \alpha = \frac{2}{Q_a} \cdot \frac{\beta}{\beta^2 - 1} \quad (9)$$

The vector diagram of  $\bar{a}$  is given in Fig. 5.

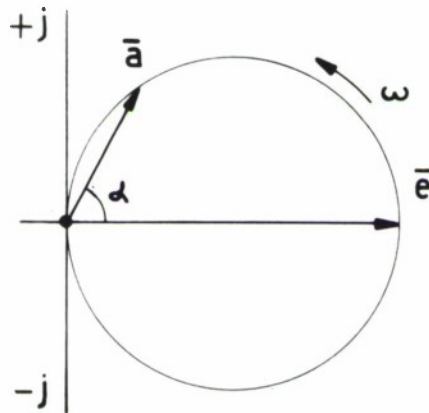


Fig. 5. Vector Diagram of the Bridged T

### 1.3 The $\bar{c}$ -circuit

The  $\bar{c}$ -circuit is a phase shifter that must produce a phase shift of  $90^\circ$  with respect to the original signal at the frequency  $f_0$ . For other frequencies, the phase angle, indicated by  $\gamma$ , should be equal to the phase angle  $\alpha$  of the  $\bar{a}$ -circuits. There are several circuits that meet these conditions; the two most useful of these will be described here.

1.3.1 The RC Phase Shifter. Figure 6 gives the diagram of the RC Phase Shifter with  $k$  indicating a factor between 0 and 1. This factor is needed to obtain a complete phase-equality with one of the given  $\bar{a}$ -circuits. In this circuit the frequency, where  $\omega R_3 C_3 = 1$ , is not equal to  $f_0$  but differs from that frequency by a factor  $\epsilon$ .



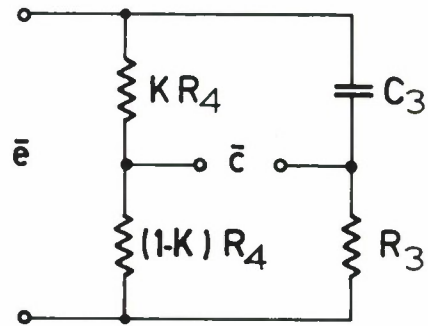


Fig. 6 The RC Phase Shifter

The factor  $\epsilon$  can be defined as

$$\epsilon = \omega_0 R_3 C_3 \quad (10)$$

The complex output voltage  $\bar{c}$  is given by

$$\frac{\bar{c}}{\bar{e}} = \frac{1}{1 + j \epsilon \beta} - k \quad (11)$$

The phase angle  $\gamma$  between  $\bar{c}$  and  $\bar{e}$  is given by

$$\text{tg } \gamma = \frac{\epsilon \beta}{k(1 + \epsilon^2 \beta^2) - 1} \quad (12)$$

The vector diagram of  $\bar{c}$  is given in Fig. 7.

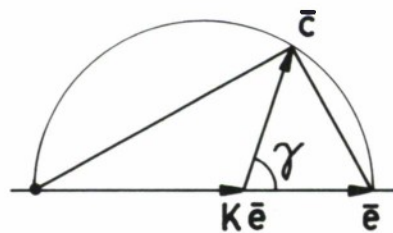


Fig. 7 Vector Diagram of the RC Phase Shifter

1.3.2 The LC Phase Shifter. Figure 8 gives the circuit diagram for the LC Phase Shifter.

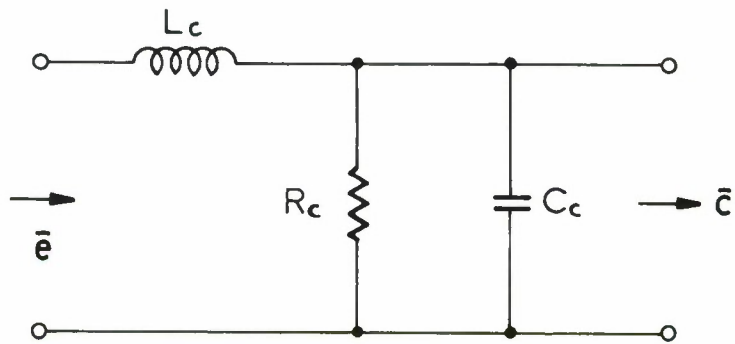


Fig. 8 The LC Phase Shifter

The condition for  $90^\circ$  phase shift at the frequency  $f_o$  is

$$\omega_o^2 L_c C_c = 1 \tag{13}$$

The quality factor  $Q_c$  of this circuit will be introduced as

$$Q_c = \omega_o R_c C_c \tag{14}$$

This factor can be used to obtain equal phase shift of this circuit with one of the  $\bar{a}$ -circuits.

The complex output voltage  $\bar{c}$  is given by

$$\frac{\bar{c}}{\bar{e}} = \frac{1}{1 - \beta^2 + j \frac{\beta}{Q_c}} \tag{15}$$

[REDACTED]

The phase angle  $\gamma$  is given by

$$\text{tg } \gamma = \frac{1}{Q_c} \cdot \frac{\beta}{\beta^2 - 1} \quad (16)$$

#### 1.4 Condition for Equal Phase

To obtain a single line, and not an ellipse, on the oscilloscope screen, the two signals  $\bar{a}$  and  $\bar{c}$  should have a phase difference of  $0^\circ$  or  $180^\circ$  when they are applied to the horizontal and vertical deflection systems. This condition is covered by the equation

$$\text{tg } \alpha = \text{tg } \gamma \quad (17)$$

for all frequencies. With this equation, the variable parameters in the different  $\bar{a}$  and  $\bar{c}$ -circuits can be solved, since they are the factors  $n$ ,  $Q_a$ ,  $k$ ,  $\epsilon$ , and  $Q_c$ . (Eqs. (4), (9), (12), and (16) refer).

#### 1.5 Display

By feeding the signal  $\bar{a}$  to the horizontal and  $\bar{c}$  to the vertical amplifier of an oscilloscope, a straight line appears on the screen, which makes an angle  $\phi$  with the vertical. With equal sensitivity of both channels this angle  $\phi$  is given by

$$\text{tg } \phi = \frac{\bar{a}}{\bar{c}} \quad (18)$$

Substituting the equations for  $\bar{a}$  and  $\bar{c}$  as functions of  $\beta$ , the inclination angle  $\phi$  can be found as function of  $\beta$ . By a proper choice of one of the parameters mentioned above, this function can be given some symmetry and linearity as will be seen later in Section 1.6.

The following sections give some examples of useful combinations of  $\bar{a}$  and  $\bar{c}$  circuits as was shown in Fig. 1.

1.5.1 Combination of Wien Bridge and RC-Bridge. Equation (17) must be applied to Eqs. (4) and (12), giving

$$(n + 2) \frac{\beta}{\beta^2 - 1} = \frac{\epsilon \beta}{k(1 + \epsilon^2 \beta^2) - 1} \quad (19)$$

Solving this equation for all values of  $\beta$  yields

$$n = \frac{(\epsilon - 1)^2}{\epsilon} \quad (20)$$

$$k = \frac{1}{\epsilon^2 + 1} \quad (21)$$

For every chosen value of  $\epsilon$  one value for  $n$  and  $k$  can be found, so that the circuits can be realized. The choice of  $\epsilon$  allows some symmetry to be introduced.

Substituting (20) and (21) in (3) and (11) gives the values of  $\bar{a}$  and  $\bar{c}$  as functions of  $\beta$ . Substitution of these values in (18) gives

$$\text{tg } \phi = \frac{(\epsilon - 1)^2 (\beta^2 - 1)}{\epsilon^2 + \beta^2} \quad (22)$$

1.5.2 Combination of Bridged-T and RC-Bridge. Equations (9) and (12) have to be substituted in Eq. (17), which gives

$$\frac{2}{Q_a} \cdot \frac{\beta}{\beta^2 - 1} = \frac{\epsilon \beta}{k(1 + \epsilon^2 \beta^2) - 1} \quad (23)$$

Solving this equation for all values of  $\beta$  yields

$$Q_a = \frac{2 \epsilon}{\epsilon^2 + 1} \quad (24)$$

$$k = \frac{1}{\epsilon^2 + 1} \quad (25)$$

Substituting these values in (8) and (11), and substituting the latter equations in (18), gives

$$\text{tg } \phi = \frac{(\epsilon^2 + 1)(\beta^2 - 1)}{\epsilon^2 + \beta^2} \quad (26)$$

In the same way as mentioned in Section 1.5.1, the factor  $\epsilon$  is still free to give this function the desired linearity and symmetry.

1.5.3 Combination of Bridged-T and LC Phase Shifter. Here, the parameters can be solved by substitution of the functions (9) and (16) in Eq. (20) to give

$$\frac{2}{Q_a} \cdot \frac{\beta}{\beta^2 - 1} = \frac{1}{Q_c} \cdot \frac{\beta}{\beta^2 - 1} \quad (27)$$

with the solution

$$Q_a = 2 Q_c \quad (28)$$

Substitution of Eqs. (8) and (15) in (18) gives, with (28)

$$\text{tg } \phi = 1 - \beta^2 \quad (29)$$

This function shows no parameter: it is independent from  $Q_a$  and  $Q_c$ . A plot of this function is given in Fig. 9, which shows the non-linearity of this type of frequency indicator.

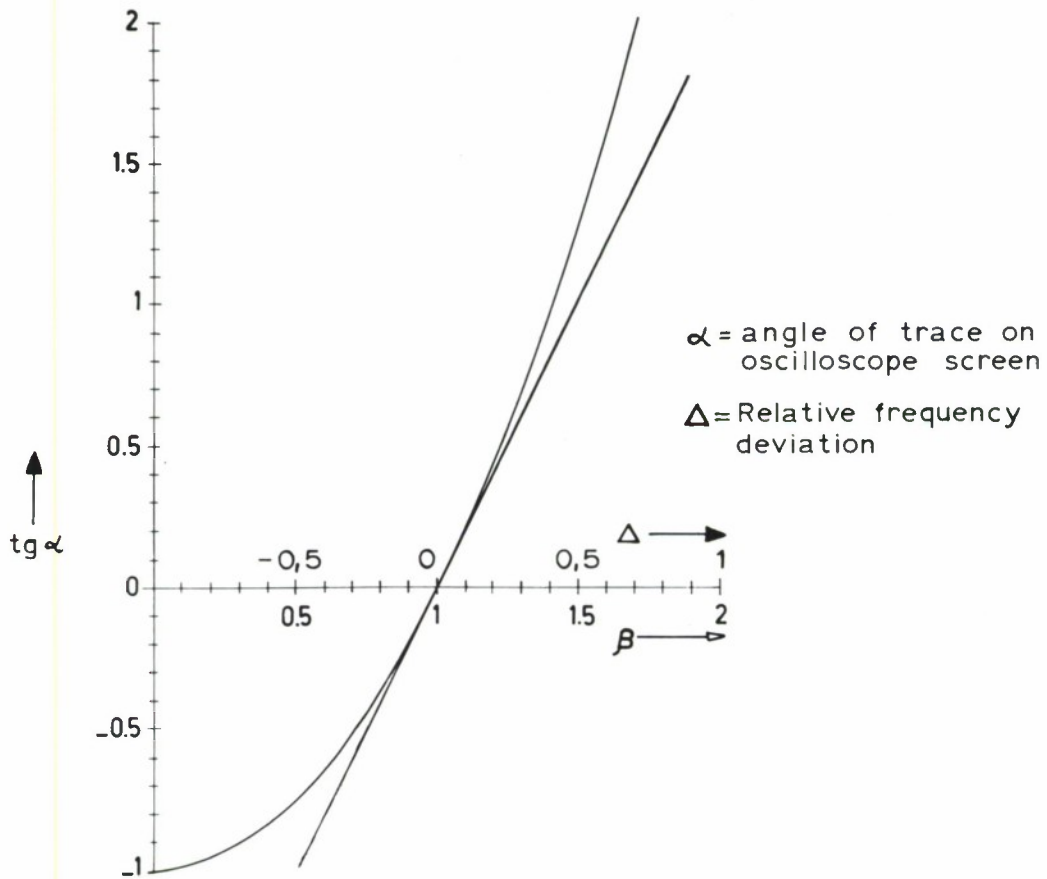


Fig. 9 Visual Display Response Curve of LC Discriminator

## 1.6 Symmetry

In order to find the right value for  $\epsilon$  in the functions (22) and (26), the relative frequency deviation  $\Delta$  will be introduced, defined as follows: the frequency  $f$  can be related to the central frequency  $f_0$  as

$$f = f_0 + \Delta f_0 \quad (30)$$

introducing  $\Delta$  as

$$\Delta = \frac{\Delta f_0}{f_0} \quad (31)$$

$\Delta$  is a factor between -1 and +1, or sometimes even higher than +1.

Equation (1) yields

$$\beta = 1 + \Delta \quad (32)$$

Now, the condition for symmetry will be satisfied as follows, when

$$\Delta = +\Delta_1, \quad \text{tg } \phi = +T$$

and, when

$$\Delta = -\Delta_1, \quad \text{tg } \phi = -T$$

Applying this principle to the functions (22) and (26),  $\epsilon$  can be solved to the value that gives symmetry to the  $\phi$  vs.  $\Delta$  curve.

It will be found for both functions that

$$\epsilon^2 = 3 - \Delta^2 \quad (34)$$

Obviously a complete symmetry for all values of  $\Delta$  cannot be realized, as the required value for  $\epsilon$  still depends on  $\Delta$ . But, when  $\Delta^2 \ll 3$ , it will be found that

$$\epsilon \approx \sqrt{3} \quad (35)$$

The remaining unknown parameters in the circuits can now be solved from Eqs. (20), (21), (24), and (28)

$$\begin{aligned} n &= 0.31 \\ k &= 1/4 \\ Q_a &= 1/2 \sqrt{3} \\ Q_c &= 1/4 \sqrt{3} \end{aligned} \quad (36)$$

The curves giving the display angle on the oscilloscope screen versus the relative frequency deviation  $\Delta$  for the different combinations of circuits can be drawn from Eqs. (22) and (26) substituting  $\epsilon = \sqrt{3}$  and  $\beta = 1 + \Delta$ .

Referring to the combination of the Wien Bridge and the RC Bridge: Eq. (22)

$$\text{tg } \phi = 0.536 \Delta \frac{\Delta + 2}{\Delta^2 + 2\Delta + 4} \quad (37)$$

Referring to the combination of the Bridged-T and the single RC-Bridge: Eq. (26)

$$\operatorname{tg} \phi = 4 \Delta \frac{\Delta + 2}{\Delta^2 + 2 \Delta + 4} \quad (38)$$

These functions are the same, apart from a constant factor that only influences the sensitivity of the indicator.

The general curve

$$\operatorname{tg} \phi = \frac{\Delta (\Delta + 2)}{\Delta^2 + 2 \Delta + 4} \quad (39)$$

is drawn in Fig. 10, and shows the good linearity in the vicinity of  $\Delta = 0$  compared to Fig. 9.

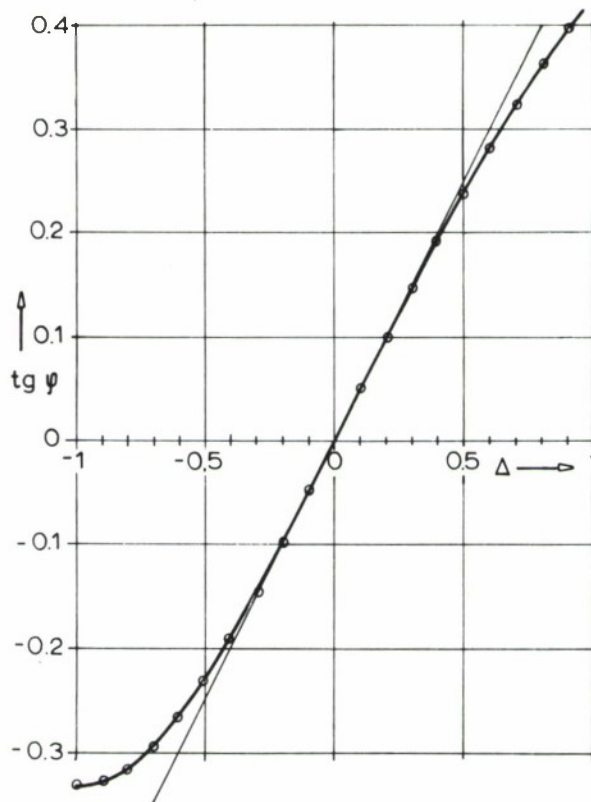


Fig. 10 Visual Display Response Curve of Symmetrified RC Discriminator



## 1.7 Conclusion

A symmetrical indication of frequency deviations as high as half the central frequency ( $\Delta < 0.5$ ) can be obtained by combination of a "null-network" with a RC phase shifter. Indication is still possible for higher frequency deviations but the symmetry will be poor. The null-network can be composed only of resistors and capacitors.

The sensitivity of the indicator can be changed between wide limits by changing the gain of the amplifiers in the two channels.

When only weak signals are available in a noisy background and when the frequency deviations are relatively small, the Wien-Bridge will give no clear indication. In this case, the Bridged-T can be used in the  $\bar{a}$ -channel and the LC phase shifter in the  $\bar{c}$ -channel, both with high Q-values, bearing in mind Eq. (28)  $Q_a = 2 Q_c$ . For small frequency changes ( $\Delta < 0.1$ ), the symmetry of this type of discriminator will be good enough, as can be seen from Fig. 9.

## PART 2

### REGISTRATION ON A DC - RECORDER

#### 2.1 Principles

The same circuits that are described in Part 1 can be used to construct a discriminator, which produces a DC voltage proportional (between certain limits) to the frequency deviation  $\Delta$  similar to a FM demodulator.

2.1.1 Division. When the signal  $\bar{a}$  is divided by the signal  $\bar{c}$  with the aid of some electronic divider, a DC component will be obtained which is approximately proportional to the frequency deviation  $\Delta$  and independent of the amplitude of the original signal. The same parameter values that are found in Part 1 will also give a symmetric frequency deviation scale in this case. However, the complexity of a 4-quadrant electronic divider is a great drawback for the practical use of this type of discriminator.

2.1.2 Multiplication. Electronic multiplication of the two signals  $\bar{a}$  and  $\bar{c}$  gives also a DC voltage, which is a monotone function of the frequency deviation  $\Delta$  but it is also proportional to the square of the original signal voltage. An amplitude limiter is required to keep the input voltage  $|\bar{e}|$  constant. A proper choice of the circuit parameters here leads also to a symmetrical frequency deviation scale. These factors must be the same as in Part 1 (see Eq. (36)) except for

$$\epsilon = 1/3 \sqrt{3}$$

and

$$k = 3/4$$

Possible multipliers are:

1. Hall generator multiplier
2. Square law diode multiplier
3. Pentagrid converter tube multiplier, etc.

2.1.3 Rectification. The simplest way to obtain a frequency dependent DC voltage is to rectify the signal  $|\bar{a}|$  with a phase sensitive detector, using the signal  $\bar{c}$  only as a phase reference. The rectifier will produce a DC voltage proportional to  $|\bar{a}|$  as long as  $\bar{a}$  and  $\bar{c}$  are in phase, and proportional to  $-|\bar{a}|$  when  $\bar{a}$  and  $\bar{c}$  are in phase opposition. In order to obtain an output voltage at the discriminator that is dependent only on the frequency of the signal, an amplitude limiter is needed to reduce the amplitude variations of the original signal.

Figure 11 gives the circuit diagram of a phase sensitive detector on which the balanced DC output voltage is indicated by D. In order to raise the voltage level of D, the resistors r, in series with the diodes, serve to increase the impedance of the conducting branch of the diode bridge.

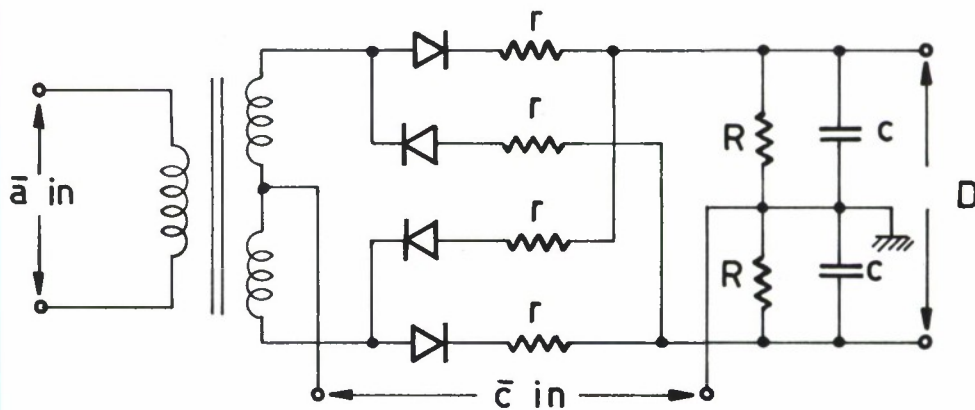


Fig. 11 Phase Sensitive Detector

## 2.2 Analysis of Discriminator with Rectifier

The principle mentioned in Section 2.1.3 will be considered more in detail. Figure 12 gives a block diagram of this type of discriminator.

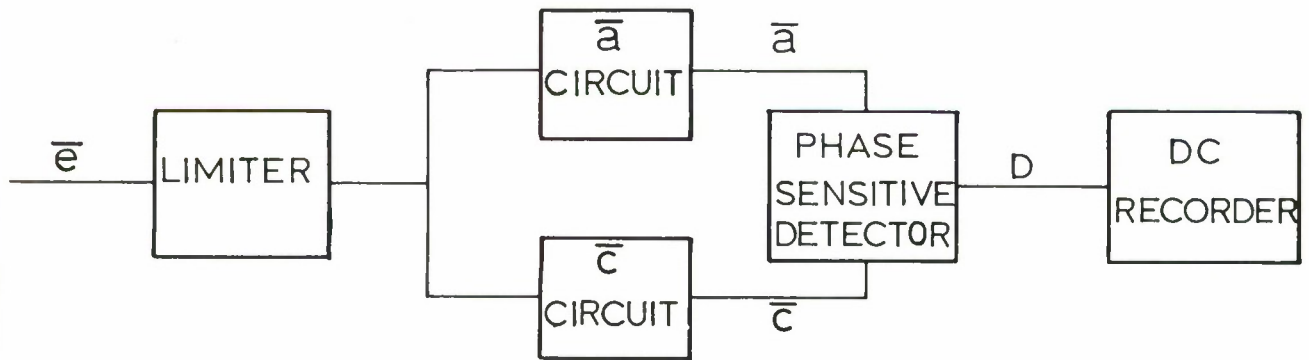


Fig. 12 Block Diagram of DC Discriminator

2.2.1 Response Curve. The output voltage  $D$  is proportional to  $\pm |\bar{a}|$  ; the sign depends on the phase between  $\bar{a}$  and  $\bar{c}$ . The curve for  $D$ , as a function of the relative frequency deviation  $\Delta$ , can be derived from Eqs. (3) or (8), depending on the type of  $\bar{a}$ -circuit that has been chosen. As an example, Eq. (8) has been taken, substituting

$$\bar{e} = 1, \quad Q_a = 1$$

and

$$\beta = \Delta + 1$$

Hence

$$\bar{a} = \frac{1}{1 - \frac{2j}{\Delta} \frac{\Delta + 1}{\Delta + 2}} \quad (40)$$

UNCLASSIFIED

The curve  $D = \pm \left| \bar{a} \right|$  is drawn in Fig. 13.

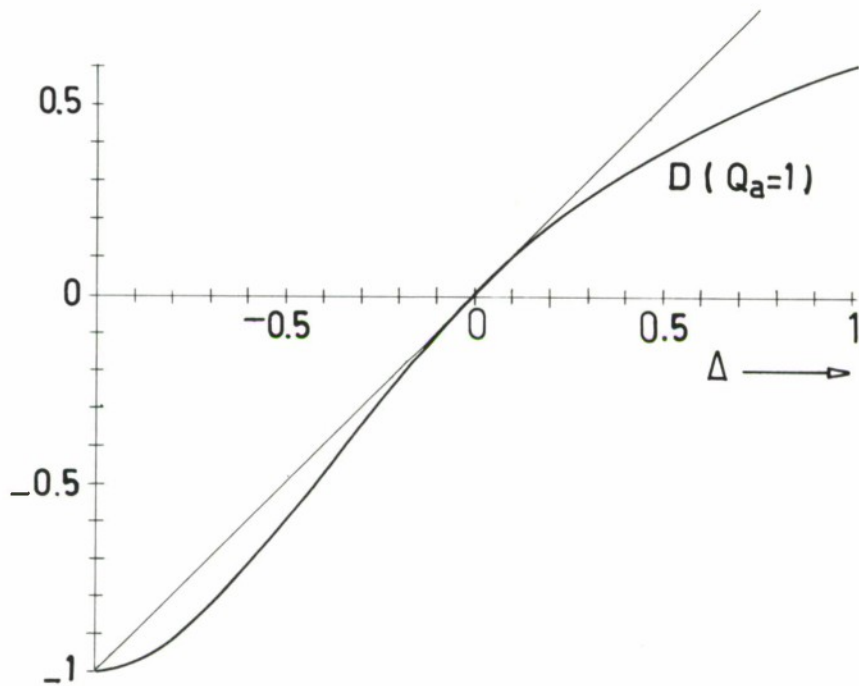


Fig. 13 Response Curve of Discriminator: DC Voltage at Recorder as a Function of  $\Delta$

Other curves for other values of  $Q_a$ , or derived from Eq. (3) with different values of the parameter  $n$ , have all about the same general shape, but the slopes at  $\Delta = 0$  are different.

**2.2.2 Sensitivity.** The sensitivity of the discriminator is defined by the ratio between the output voltage  $D$  and the relative frequency deviation  $\Delta$  as

$$S = \frac{D}{\Delta} \quad (41)$$

As the output voltage  $D$  is proportional to  $\left| \bar{a} \right|$  (or  $-\left| \bar{a} \right|$ ), Eq. (41) can be written as

$$S = \left| \frac{\bar{a}}{\Delta} \right| \quad (42)$$

Solving this equation for  $\Delta \rightarrow 0$  gives the sensitivity  $S_o$  at this point of the curve. The input signal  $\bar{e}$  of the discriminator is assumed to be 1 v.

For the Wien-Bridge, the sensitivity can be found from Eq. (3)

$$S_o = \frac{2n}{(n+2)^2} \quad (43)$$

For the Bridged-T, Eq. (8) has to be taken, giving

$$S_o = Q_a \quad (44)$$

The maximum of Eq. (43) will be found when  $n = 2$  and has the value  $S_{o\max} = 0.25$ . Equation (44), however, shows no maximum but increases at any value that can be given to  $Q_a$ . Therefore, the Bridged-T can definitely give a higher sensitivity to the discriminator than the Wien-Bridge circuit. \*

---

\*For this reason, the Wien-Bridge will be used only for the CRT display indicator of Part 1 and in those cases where the use of coils is prohibitive or undesirable for some reason, as for instance:

1. The inductance of the coils is temperature dependent; a change in temperature will cause a shift of the center frequency. The error in indication, arising in this way, increases with increasing sensitivity.
2. The inductance of the coils is also dependent on the level of the signal above a certain value. This also causes a shift in central frequency and distortion at higher signal amplitudes.
3. The LC-circuits are more expensive, heavier, and bigger than the RC-circuits.

2.2.3 Impedance of  $\bar{a}$  and  $\bar{c}$ -circuits. When two networks are fed in parallel from one source, it is advisable, from the point of view of energy distribution, to have the impedance of the two networks equal. When feeding the Bridged-T and the LC phase shifter in parallel from the same amplifier, their impedance can be equalized by a proper choice of the ratio  $\frac{L_c}{L_a}$ . (Ref. Figs. 4 and 8).

The impedance of the Bridged-T at the frequency  $\omega_o$  is:

$$\left| \bar{Z}_{ao} \right| = \frac{\omega_o L_a}{2} \sqrt{Q_a^2 + 1} \quad (45)$$

The impedance of the LC phase shifter at the same frequency is

$$\left| Z_{co} \right| = \frac{\omega_o L_c}{\sqrt{Q_c^2 + 1}} \quad (46)$$

These impedances are equal when

$$\frac{L_c}{L_a} = \frac{Q_a^2 + 2}{4} \quad (47)$$

since  $Q_a = 2Q_c$ . (Eq. 28)

Because the ratio of  $L_c$  and  $L_a$  does not otherwise influence the response curve of this discriminator, the choice of their values is free. Hence, Eq. (47) can be helpful for the final design of the circuits.

### 2.3 Extension of the Frequency Range

The center frequency of the discriminator has a fixed value that cannot easily be changed. When the frequency deviation from another mean value has to be recorded, the other mean frequency has to be converted to the center frequency of the discriminator.

Because of its ability to suppress the original signals and to produce only modulation products, out of which the fundamental mode can be filtered easily, a ring modulator may be used as converter.

The unknown frequency  $f_1$  will be mixed with the frequency of a signal generator  $f_1 \pm f_0$  to produce the discriminator center frequency  $f_0$ . It is important that the frequency of the signal generator is constant compared with the frequency of the signal to be measured. A crystal controlled oscillator can be used if needed.

A block diagram of the complete discriminator is given in Fig. 14.

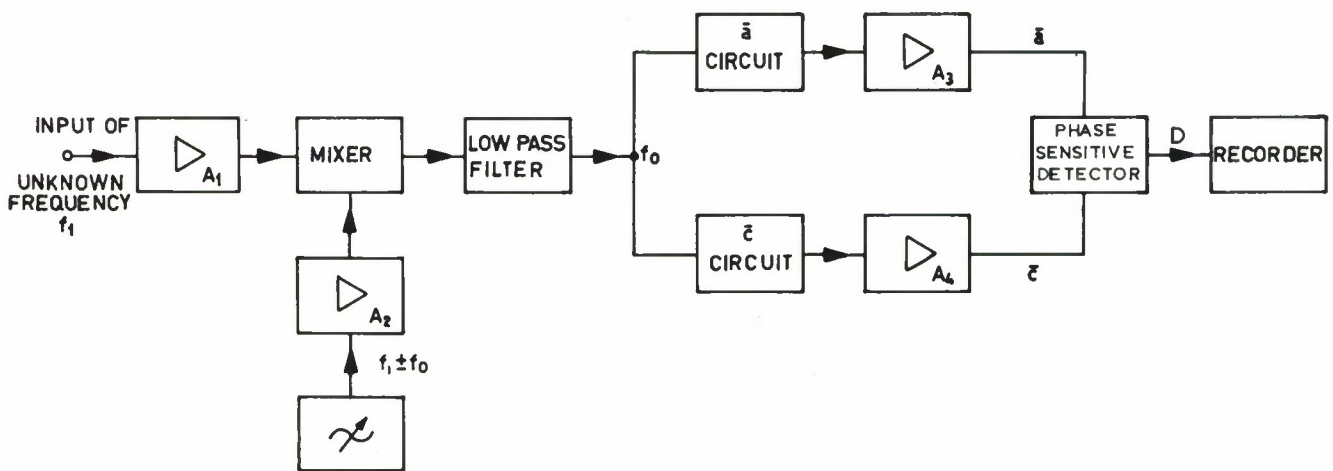


Fig. 14 Block Diagram of Complete Frequency Deviation Recorder

PART 3

SOME REALIZED CIRCUITS

3.1 Indicator with RC Networks (Fig. 15)

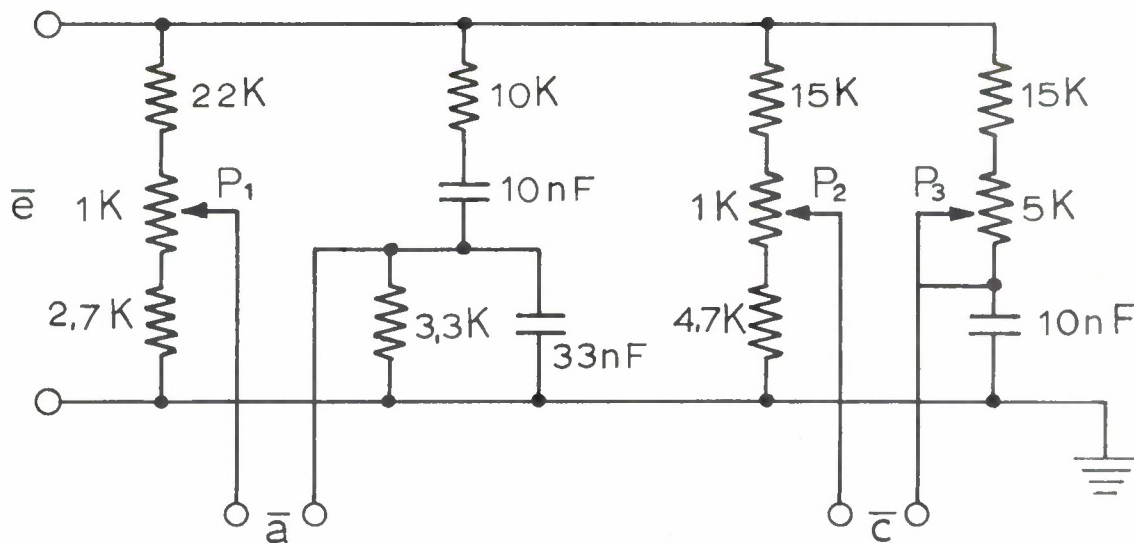


Fig. 15 Practical Circuit for RC Discriminator:  $f_o = 1.5 \text{ Kc}$

The RC Network is constructed following the principles of Figs. 2 and 6 and using Eqs. (2), (10), (35), and (36) to calculate the actual values of the resistors and condensers. The central frequency was intended to be about 1.5 kc.

The circuit has been built up with standard components with tolerances of 10%. Therefore, potentiometers are inserted on critical points:

$P_1$  - serves to have a complete zero for  $\bar{a}$  at the frequency  $f_o$

$P_2$  - brings the factor k to the right value. Eqs. (20) and (21)

$P_3$  - brings the factor  $\epsilon$  to the right value. Eqs. (20) and (21)

$P_2$  and  $P_3$  are adjusted to keep the phase difference between  $\bar{a}$  and  $\bar{c}$  exactly on  $0 \pm 180^\circ$  for all frequencies. This is a matter of repetitive correction of  $P_2$  and  $P_3$  at different frequencies until the final settings are found.

3.1.1 Calibration. This circuit has been calibrated with the  $\bar{a}$ -channel to the horizontal and the  $\bar{c}$ -channel to the vertical deflection plates of an oscilloscope. The sensitivity ratio between the two channels has been varied, and, for each ratio, the frequencies are noted for inclination angles of  $-45^\circ$  and  $+45^\circ$ . The results are shown in Table 1. The resultant central frequency  $f_0$  is 1555 cps.

TABLE 1

Sensitivity ratio $\frac{\bar{a}\text{-channel}}{\bar{c}\text{-channel}}$	Frequencies for inclination angles of		Frequency differences $\Delta f$ for inclination angles of	
	$-45^\circ$	$+45^\circ$	$-45^\circ$	$+45^\circ$
500	1544	1566	- 11	+ 11
200	1527	1583	- 28	+ 28
100	1497	1612	- 58	+ 57
50	1435	1673	- 120	+ 118
20	1250	1850	- 305	+ 295
10	920	2160	- 635	+ 605
5	0	2930	-1555	+1375

3.1.2 Conclusion. It appears from Table 1 that the symmetry is excellent for relative frequency deviations  $\Delta$  up to 0.2 ( $\Delta f_o \approx 300$  cps) and good for  $\Delta$  up to 0.5 ( $\Delta f_o \approx 800$  cps). This is in agreement with the theoretical curve of Fig. 10. The sensitivity ratio of 500 makes an indication of 1 cps in 1600 cps clearly possible. For still higher sensitivities, the signal should be properly filtered to reduce noise and harmonics that otherwise might blur the horizontal component of the picture.

3.2 Indicator with LC-Networks (Fig. 16)

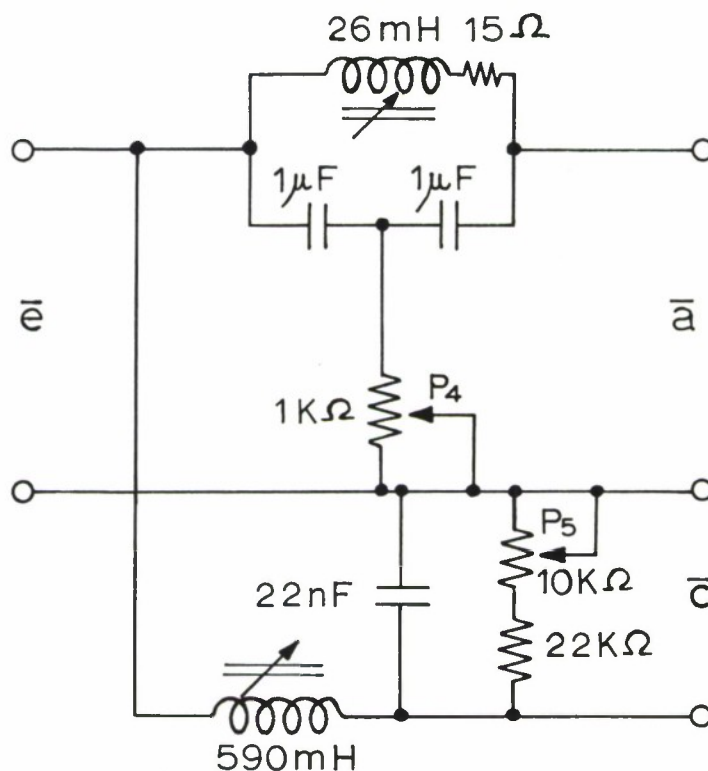


Fig. 16 Practical Circuit for LC Discriminator:  $f_o$  1.5 Kc

This circuit is constructed from the diagrams of Figs. 4 and 5. The actual values of the components are calculated using Eqs. (5), (6), (7), (13), (14), (28), and (47). The designed central frequency was 1.4 kc.

The resistor  $r$  (Fig. 4) brings the quality factor  $Q_a$  of the Bridged-T to a value of 10. Then, the other resistor  $R$  should be 575 ohms.

According to Eq. (47), it is found

$$L_c = L_a \frac{Q_a^2 + 2}{4} = 26 \frac{102}{4} = 660 \text{ mh}$$

Then, Eq. (13) prescribes the value for  $C_c$  being 20000 pf. The nearest standard value of 22000 pf has been chosen reducing  $L_c$  to 590 mh.

Equation (28) gives the quality factor  $Q_c$  for the Phase Shifter

$$Q_c = 1/2 Q_a = 5$$

Then, Eq. (14) gives the value for  $R_c$  of 28.5 k ohm.

Variable resistors  $P_4$  and  $P_5$  have been placed in the circuit to obtain a sharp trace on the oscilloscope at all frequencies:  $P_4$  serves to reduce  $|\bar{a}|$  to zero at the frequency  $f_0$ . The circuit is regulated for all other frequencies with  $P_5$  and the tuning lug of the 590 mh coil. This procedure requires a repeated alternative setting of coil resistor to find the combination that causes a fine trace on the screen at all frequencies.

3.2.1 Calibration. The circuit has been calibrated in the same way as described in Section 2.2.1. The central frequency was found to be 1430 cps. See Table 2.

TABLE 2

Sensitivity ratio $\frac{\bar{a}\text{-channel}}{\bar{c}\text{-channel}}$	Frequency in cps for inclination angle of		Frequency difference $\Delta f_o$ in cps for inclination angles of	
	$-45^\circ$	$+45^\circ$	$-45^\circ$	$+45^\circ$
1000	1429.3	1430.7	- 0.7	+ 0.7
500	1428.5	1431.4	- 1.5	+ 1.4
200	1426.5	1433.4	- 3.5	+ 3.4
100	1423.0	1436.8	- 7.0	+ 6.8
50	1416.0	1443.5	-14.0	+13.5
20	1395	1464.5	-35	+34
10	1359	1499	-71	+69
5	1285	1570	-145	+140
2	1020	1760	-410	+330
1	0	2030	-1430	+600

3.2.2 Conclusion. The sensitivity of this discriminator is, for the same amplifier gain ratios, evidently about 8 times higher than that of the RC-type described in Section 2.2. This will be seen by comparing the two Eqs. (22)

and (29) concerning these two types of circuits, giving

$$\frac{\text{Eq. (22)}}{\text{Eq. (29)}} = \frac{(\epsilon - 1)^2}{\epsilon^2 + \beta^2} \approx \frac{1}{7.5}$$

since  $\epsilon = \sqrt{3}$  and  $\beta \approx 1$ .

The experimental value of 1/8 agrees quite well with this theoretical value.

The advantage of the higher sensitivity of the LC indicator is compensated by the drawbacks inherent in coils as mentioned at the end of Section 2.2.2.

### 3.3 Discriminator for Magnetometer

For the measurement of the changes in the earth's magnetic field, a Rubidium Vapor Magnetometer can be used. This magnetometer generates a signal with a frequency of about 210 kc which changes with the intensity of the magnetic field at the rate of 4.66 cps per  $\gamma$  ( $1 \gamma = 10^{-5}$  G). A crystal oscillator converts this frequency to the frequency  $f_1$  (Fig. 14) between 3 and 20 kc. A stable signal generator supplies the frequency  $f_1 \pm f_0$ .

The discriminator, which has been developed to measure the frequency deviations, will be described in detail in this section.

The center frequency  $f_0$  is 1.5 kc, allowing a frequency deviation of 1 kc to be measured at each side. A complete circuit diagram is given in Fig. 17.



3.3.1 The Amplifiers. The amplifiers, indicated in the block diagram in Fig. 14 as  $A_1$  to  $A_4$ , are all the same type as described in Refs. (1) and (2). Their purpose is to drive the mixer and the detector at suitable voltage levels without loading the previous stages.

3.3.2 The Mixer. The mixer is a ready made ring modulator from "AUTELCO," "Modulator AA 22/1." (Fig. 18).

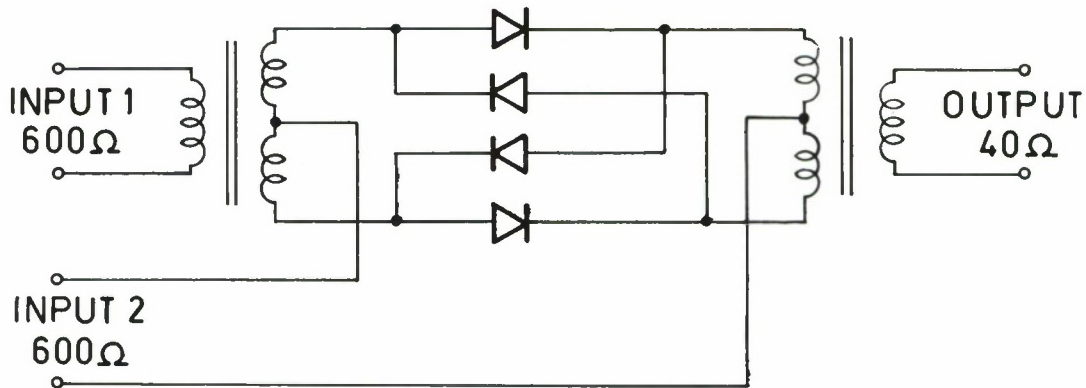


Fig. 18 "Autelco" Ring Modulator

This modulator is very well balanced; even with input frequencies of 2 and 3.5 kc, a clear 1.5 kc signal is obtained.

3.3.3 The  $\bar{a}$  and  $\bar{c}$ -circuits. It was pointed out in Section 2.2.2 that, for a high sensitivity, the Q-factor of the Bridged-T should be high. When a lower sensitivity and a larger bandwidth is required, the Q-factor has to be reduced. Therefore, a switch is provided in the circuit to change the Q-factors to the values

$$Q_{a1} = 20 \qquad Q_{c1} = 10$$

$$Q_{a2} = 6.6 \quad Q_{c2} = 3.3$$

$$Q_{a3} = 1.0 \quad Q_{c3} = 0.5$$

The two condensers of the  $\bar{a}$ -circuit are  $1 \mu\text{f}$ , giving  $L_a = 23 \text{ mh}$  for a central frequency of 1500 cps.

According to Eq. (47), when  $Q_a = 6.6$

$$L_c = 11 L_a = 250 \text{ mh}$$

and the tuning capacitor in the  $\bar{c}$ -circuit will be  $0.047 \mu\text{f}$ .

3.3.4 The  $\bar{c}$ -Amplifier  $A_4$ . Because the amplitude  $\left| \bar{c}_o \right|$  at the frequency  $f_o$  is proportional to  $Q_c$ , some precaution must be taken to keep this amplitude constant. This is done by having the resistors  $R_c$  (Fig. 8) in the  $\bar{c}$ -circuit to take part in the feed back circuit of the amplifier  $A_4$ . As the gain of the amplifier is equal to the ratio  $\frac{\text{R feedback}}{R_c}$  this gain is inversely proportional to  $Q_c$ . See Fig. 19. As a result, the output of the amplifier  $A_4$  at the frequency  $f_o$  is independent of  $Q_c$ .

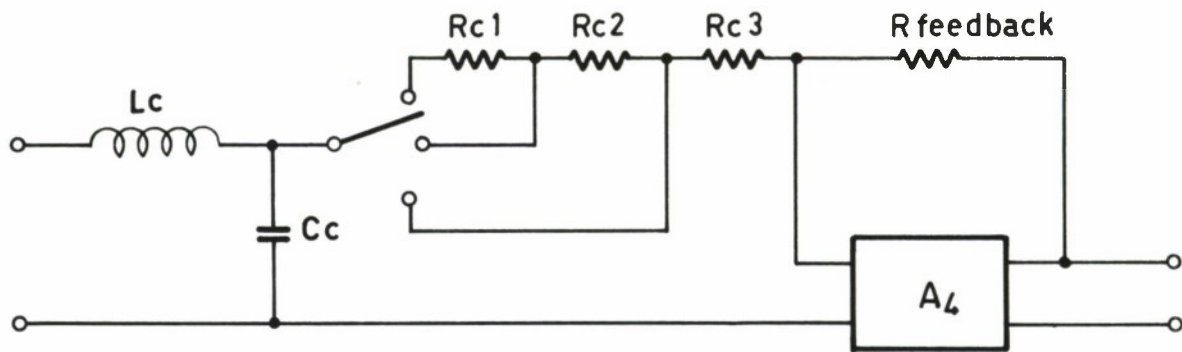


Fig. 19 Arrangement for Constant  $\left| \overline{c}_o \right|$  independent of  $Q_c$

3.3.5 The Detector. (See Fig. 11). The amplifiers, which feed the detector, are able to deliver several volts into a relatively high impedance. As the input impedance of the recorder loading the detector also is high, the detector is designed for high signal levels, using Silicon diodes OA 202 with series resistors of 10 k ohm. The RC-network is designed for a time constant of 0.03 sec.

3.3.6 Calibration. The calibration of the discriminator is performed with two signals of 1 Volt rms each; one with a frequency of 10,000 cps; the other with a variable frequency above 10 kc. It is found that the sensitivity depends on the input voltage only if this voltage is below 1 v. This is due to the limiting action of the input amplifiers and the mixer being overloaded at about 1 v.

Figures 20 and 21 give the calibration curves with the frequency difference between the two input signals as abscissae and the DC output voltage as ordinates. The curves are drawn for the three positions of the sensitivity switch: High, Medium, and Low.

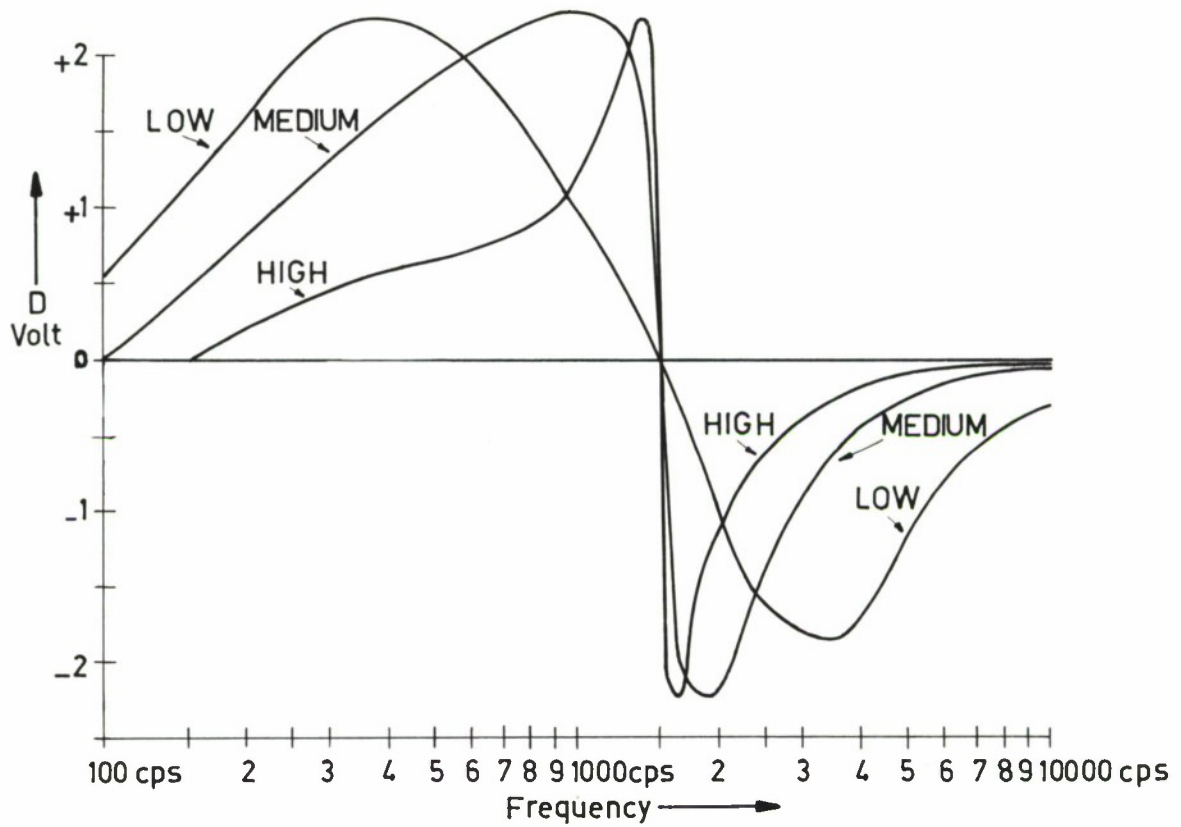


Fig. 20 Calibration Curves of Discriminator of Fig. 17

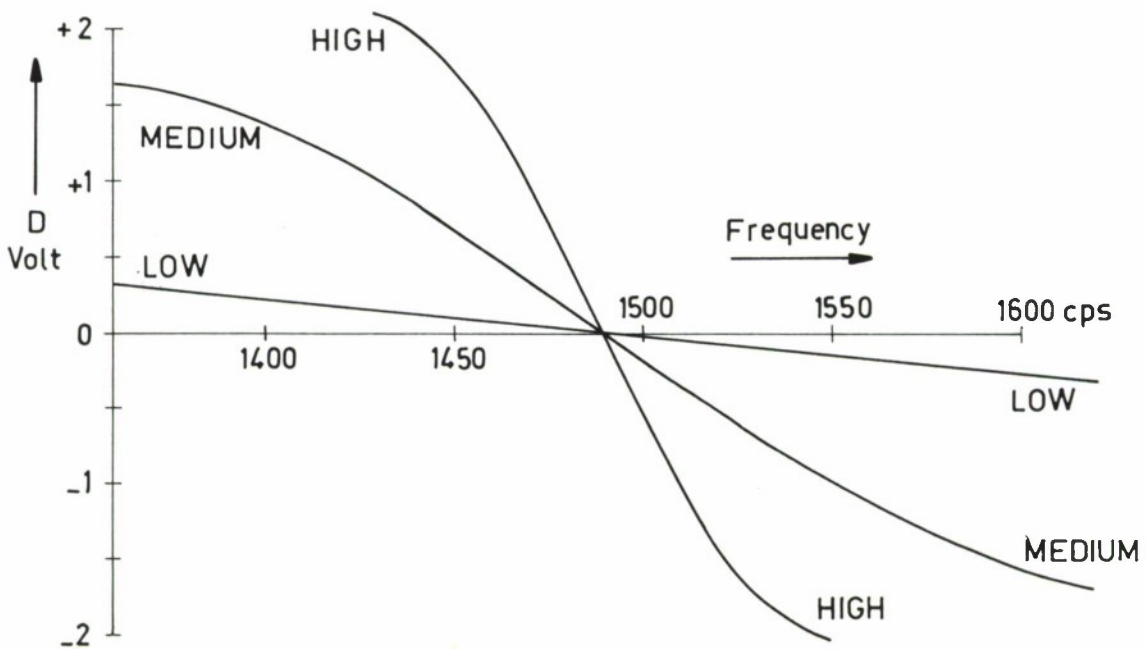


Fig. 21 Calibration Curves of Discriminator of Fig. 17

As the discriminator is intended for use with the two-channel Brush paper recorder Mark II, the conversion factors, relating the pen deflections to frequency deviations at the different sensitivities of the recorder, are given in Table 3. There is a difference in sensitivity between the central part of the recording paper and the edges due to the non-linearity of the discriminator curves. Therefore, two factors are given in the table.

TABLE 3

DISCRIMINATOR SCALE FACTORS

SENSITIVITY		FREQUENCY SHIFT IN cps/mm	
Discriminator Switch	Brush Recorder v/mm	MIDDLE	EDGES
HIGH (20 cps/v or 50 mv/cps)	0.01	0.2	0.2
	0.02	0.4	0.4
	0.05	1.0	1.1
	0.1	2.1	3.7
	0.2	5.4	-
MEDIUM (60 cps/v or 17 mv/cps)	0.01	0.6	0.6
	0.02	1.2	1.2
	0.05	3.0	3.2
	0.1	6.2	11
	0.2	16	-
LOW (420 cps/v or 2.4 mv/cps)	0.01	4.2	4.2
	0.02	8.4	9.1
	0.05	21	29
	0.1	49	-
	0.2	120	-

At the lower sensitivities of the recorder, no full scale deflection may occur. In those cases no conversion factors are given.

The highest sensitivity allows discrimination of a frequency change of 0.2 cps, corresponding to a change in the earth's magnetic field of  $0.04 \gamma$ . The lowest sensitivity allows the recording of a frequency change of about 1000 cps, corresponding to  $200 \gamma$ . For larger variations of the magnetic field, the signal generator frequency has to be changed to get the mean value of the indication near to the center line of the paper strip.

### 3.4 Discriminator for the Sound Velocity Meter

The velocity of sound waves in sea water is measured with the aid of a Sound Velocity Meter, which generates a signal with a frequency proportional to the sound velocity. The mean frequency is about 3675 cps, with a maximum deviation of 50 cps to each side, that has to be recorded as a function of depth on a X-Y recorder with the aid of a discriminator. The block diagram of the discriminator is given in Fig. 22.

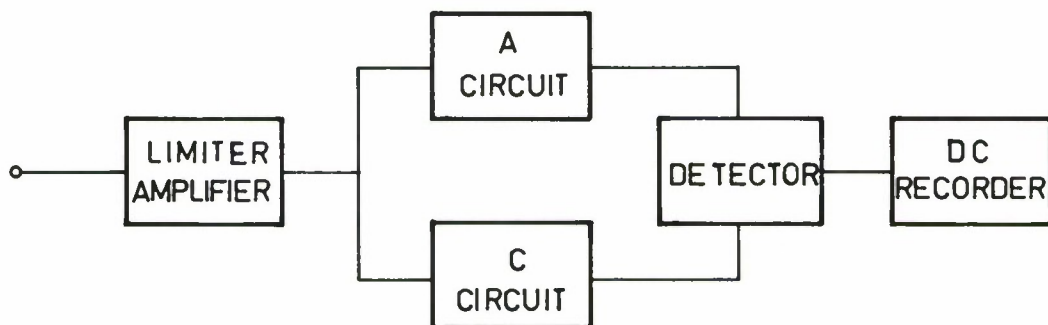


Fig. 22 Block Diagram of Sound Velocity Meter Discriminator

A complete circuit diagram is given in Fig. 23.

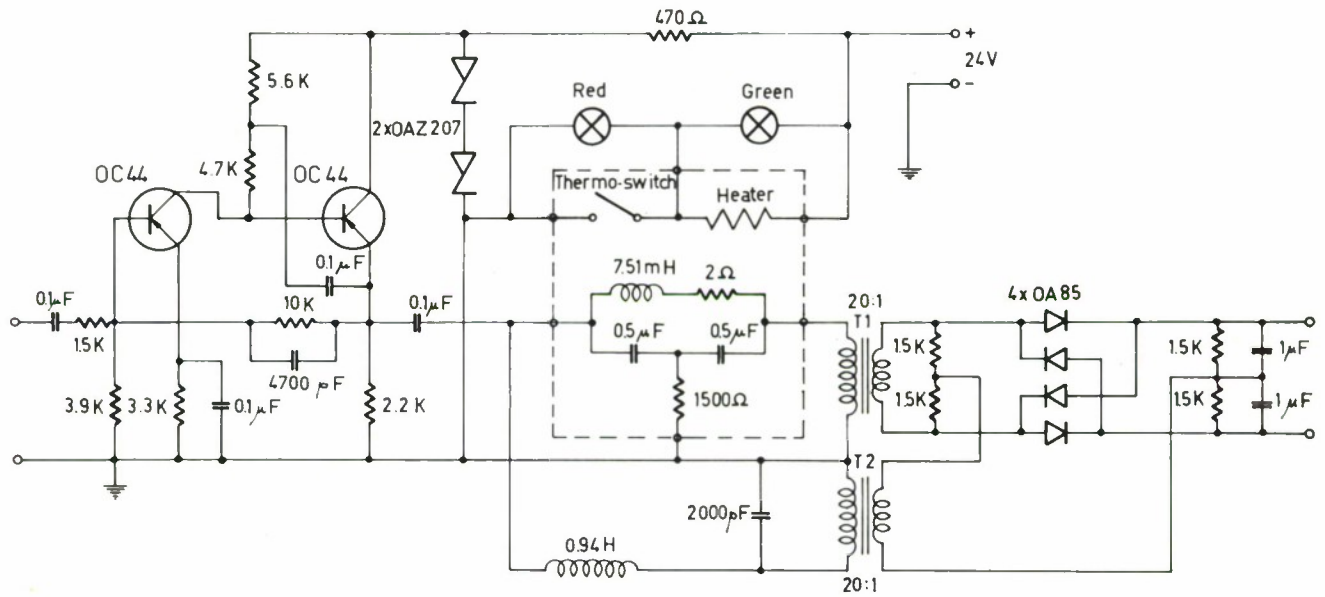


Fig. 23 Circuit Diagram of Sound Velocity Meter Discriminator

3.4.1 Limiter amplifier. The signal from the sound velocity meter is a stable square wave with a peak-to-peak value of about 4 v. As the output voltage D of the discriminator varies with the input voltage, the square wave has to be clipped. The clipping is done with an overloaded amplifier, which has a supply voltage stabilized with two Zener diodes. The influence of this limiting action is illustrated in Fig. 24, which shows the increase in sensitivity of the discriminator with increasing peak-to-peak input voltage.

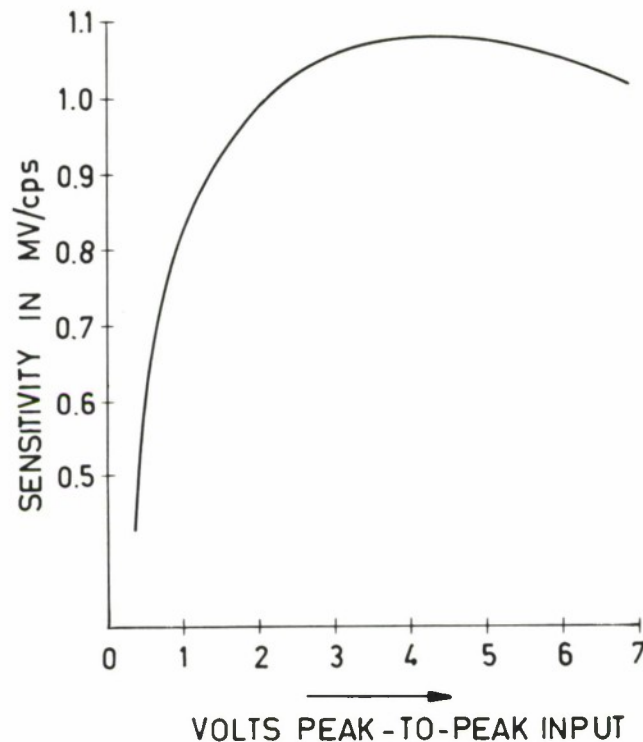


Fig. 24 Sensitivity of Discriminator as a Function of Input Signal Voltage Level

3.4.2 The  $\bar{a}$ -circuit. The resonant frequency of the Bridged-T circuit is 3670 cps. The Q factor is  $Q_a = 34$ ; it is brought to this value by the additional series resistance of 2 ohms. The capacitors are Siemens Styroflex condensers  $0.5 \mu f \pm 0.3\%$ .

3.4.3 Precision and Stability. Because one of the requirements for the discriminator is a high precision in absolute frequency indication for varying ambient temperature, the  $\bar{a}$ -circuit has been mounted in a thermostat oven of the type used for stabilizing precision Quartz oscillator crystals. The temperature is stabilized at  $65^\circ C \pm 1^\circ$ . The temperature coefficients of the different components is not known precisely, but the order of magnitude is

estimated to be:

For Styroflex capacitors

$$\frac{\Delta C}{C \cdot \Delta T} \approx - 150 \cdot 10^{-6} / ^\circ\text{C}$$

For Siemens Siferit 550 M25 with a  $\mu_g = 50$

$$\frac{\Delta L}{L \cdot \Delta T} \approx + 100 \cdot 10^{-6} / ^\circ\text{C}$$

The temperature coefficient of the resonant frequency will be found from  $\omega^2 LC = 1$  to be

$$\begin{aligned} \frac{\Delta f}{f \cdot \Delta T} &= - \frac{1}{2} \frac{\Delta C}{C \Delta T} - \frac{1}{2} \frac{\Delta L}{L \cdot \Delta T} \\ &= 75 \cdot 10^{-6} - 50 \cdot 10^{-6} = 25 \cdot 10^{-6} / ^\circ\text{C} \end{aligned}$$

when  $f_0 = 3670$  cps,

$$\frac{\Delta f}{\Delta T} = 0.1 \text{ cps } / ^\circ\text{C}^*$$

\* A change in the central frequency  $f_0$  of 8 cps was measured when the temperature changed from  $20^\circ\text{C}$  to  $60^\circ\text{C}$ , giving a temperature coefficient of

$$\frac{\Delta f}{\Delta T} = \frac{8}{40} = 0.2 \text{ cps } / ^\circ\text{C}$$

3.4.4 The  $\bar{c}$ -circuit. According to Eq. (47) the inductance  $L_c$  should be

$$L_c = L_a \frac{Q_a^2 + 2}{4}$$

With  $L_a = 7.5$  mh and  $Q_a = 34$  it is found that  $L_c = 2.2$  h

However, it appears that the load resistance  $R_c$  (Fig. 13) would be an impractically high value. In the design of this discriminator, the resistor  $R_c$  is incorporated in the load introduced by the transformer T2 and the rectifier bridge (Fig. 23).  $R_c$  was found to be about 400 k ohm.

The values of  $C_o$  and  $L_c$  are determined from Eqs. (13) and (14) when  $Q_c$ ,  $\omega_o$  and  $R_c$  are given. With  $Q_c = 17$  and  $R_c \approx 400$  k ohm it is found that

$$C_c = 2000 \text{ pf}$$

$$L_c = 0.94 \text{ h}$$

3.4.5 The Rectifier. Because of the high sensitivity of the recorder, the output voltage D should be of the order of magnitude of 10 mv. Therefore, the levels of  $\bar{a}$  and  $\bar{c}$  are stepped down by the transformers  $T_1$  and  $T_2$  by a factor 20, unloading the  $\bar{a}$  and  $\bar{c}$ -circuits from the impedance of the rectifier by a factor 400.

Because of the low signal levels, the diodes are of the germanium type, OA 85, and the load resistances are low, 1.5 k ohm, giving with the  $1 \mu$  F a condensers time constant of 1.5 ms.

3.4.6 Calibration. The discriminator has been calibrated with a square wave signal of a 4 v peak-to-peak. Figure 25 gives the DC output voltage in millivolts versus the signal frequency.

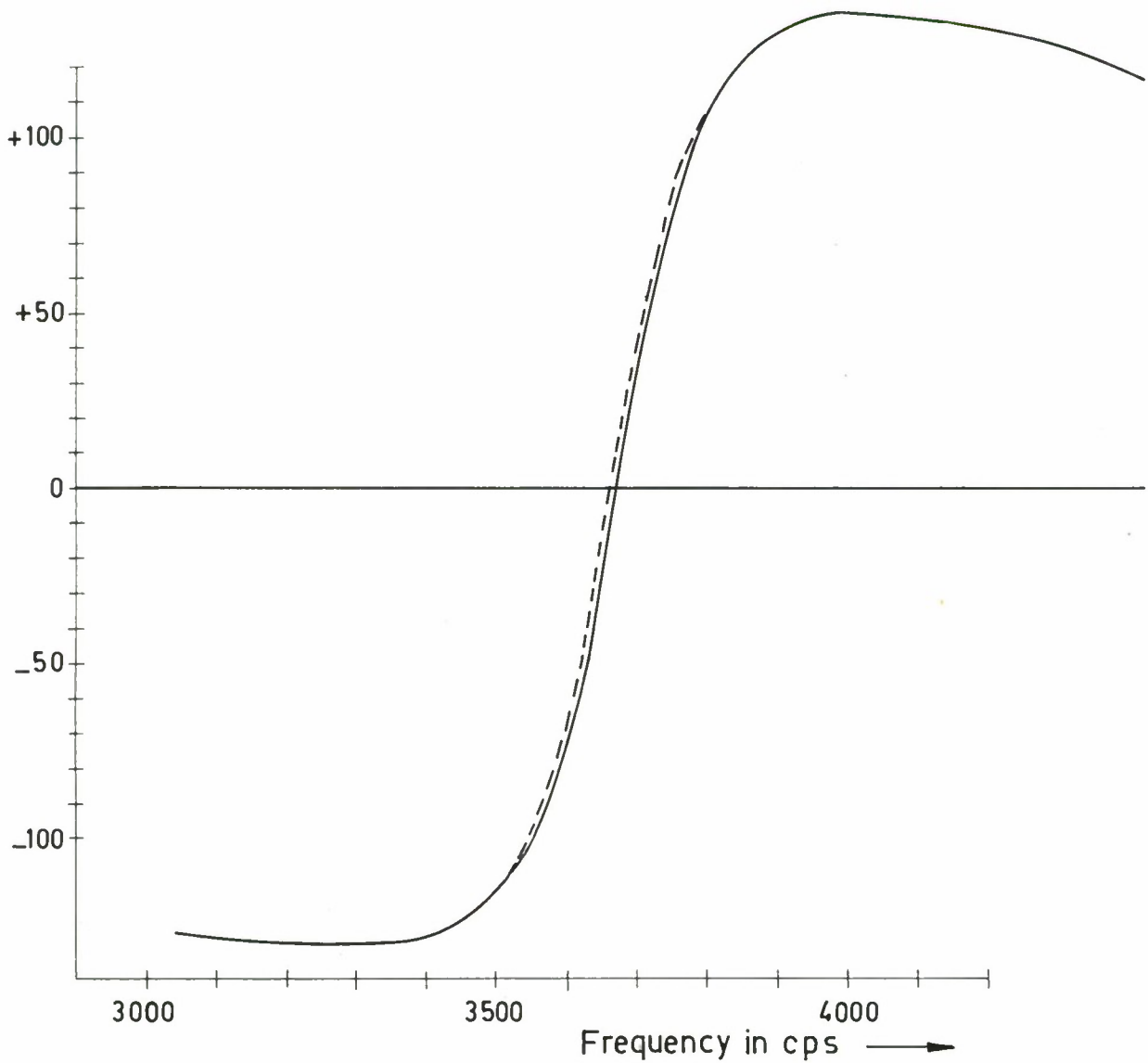


Fig. 25 Calibration Curve of Discriminator of Fig. 23

Figure 26 is an enlargement of the central, most important, part of the curve of Fig. 25.

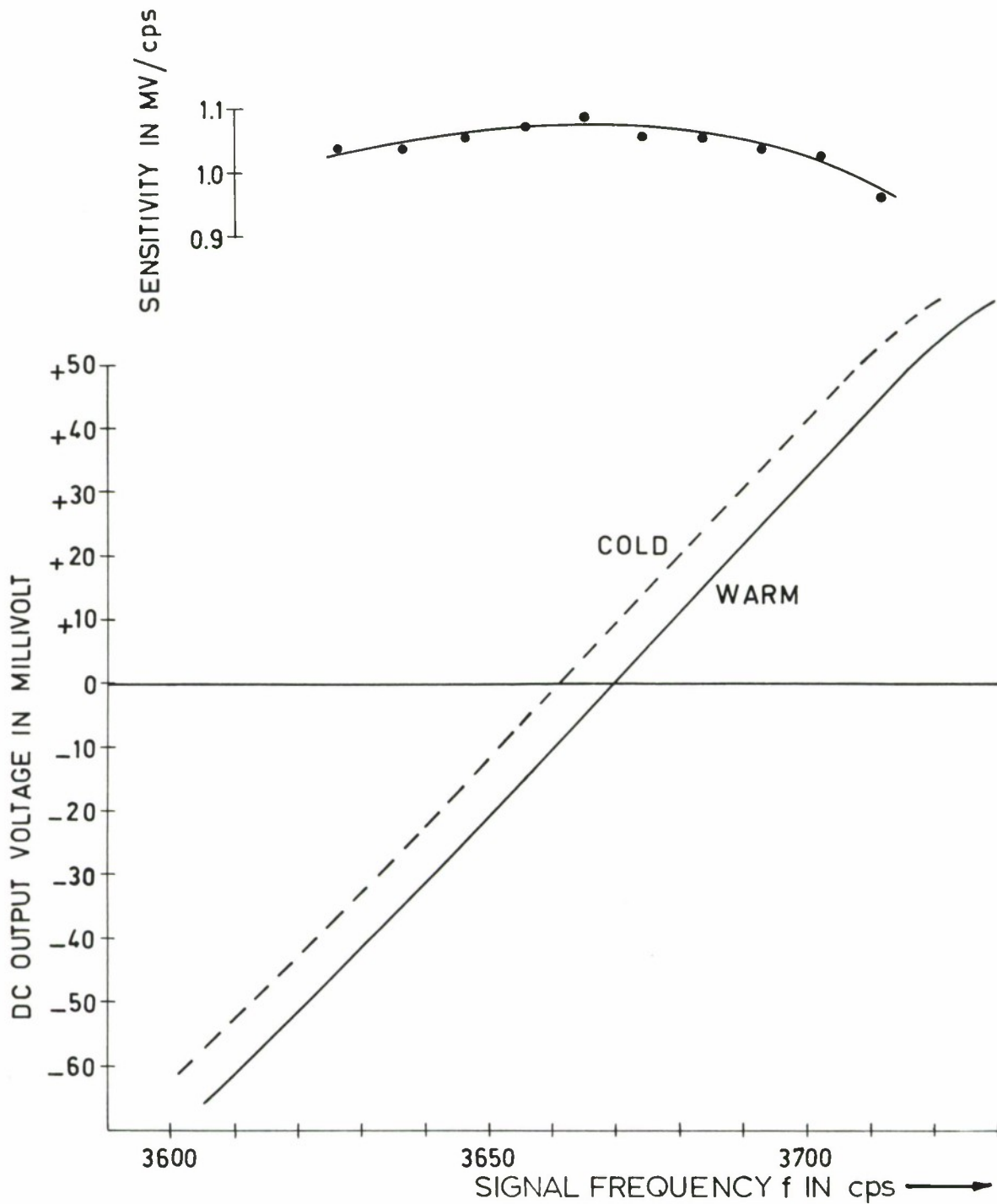


Fig. 26 Calibration Curve of Discriminator of Fig. 23

The dotted lines refer to normal room temperature: discriminator "cold." The full drawn curve is valid after an oven warm-up time of at least one hour: discriminator "warm," temperature 65°C. The sensitivity of the discriminator has been accurately measured with a frequency counter, giving the frequency with the precision of 0.1 cps.

At the top of Fig. 26, the curve for the sensitivity versus frequency is given in millivolts per cycles per second frequency change. At the central frequency 3670 cps the sensitivity is maximum:

$$S_{Do} = 1.07 \text{ mv/cps}$$

slowly decreasing at both ends of the frequency range.

#### 3.4.7 Conclusions.

1. The linearity of the discriminator curve in Fig. 26 appears to be reasonably good within the desired frequency range between 3620 and 3720 cps.
2. The short term stability gives a reproducible indication for one day within 0.3 cps, giving a precision of  $10^{-4}$ .
3. The long term stability is not well known. A difference in  $f_o$  of 1 cps has been found between one day and the next, reducing the precision to  $3 \cdot 10^{-4}$ . However, the difference may be due to an aging effect of the styroflex condensers in the  $\bar{a}$ -circuit. These condensers have a maximum working temperature of 70°C; they are heated each day from 15°C to 65°C, causing some thermal deformation. Shortly after the construction of the discriminator, there was a daily increase of  $f_o$  of

about 5 cps that decreased gradually to 1 cps per day. It may be, finally, that a stable situation has been reached.

4. The sensitivity of the instrument allows a discrimination of 0.1 cps, provided the recorder indicates a difference in DC voltage of 0.1 mv.

APPENDIX I

Derivation of the Equations.

Equation (3)

$$(1) \text{ and } (2) \quad \omega R_1 C_1 = \beta$$

$$\text{Figure 2: } \frac{\bar{a}}{\bar{e}} = \frac{j \beta n}{1 - \beta^2 + j \beta (n + 2)} - \frac{n}{n + 2}$$

$$= \frac{n}{n + 2} \cdot \frac{\beta^2 - 1}{1 - \beta^2 + j \beta (n + 2)}$$

$$= \frac{n}{n + 2} \cdot \frac{1}{-1 + j \frac{\beta}{\beta^2 - 1} (n + 2)} \quad (3)$$

Equation (12)

$$(1) \text{ and } (10) \quad \omega R_3 C_3 = \epsilon \beta$$

Figure 6: 
$$\frac{\bar{c}}{\bar{e}} = \frac{1}{1 + j \epsilon \beta} - k \tag{11}$$

$$= \frac{1 - k (1 + \epsilon^2 \beta^2) - j \epsilon \beta}{1 + \epsilon^2 \beta^2}$$

tg  $\gamma = \frac{-\epsilon \beta}{1 - k (1 + \epsilon^2 \beta^2)}$  (12)

Equation (15)

(1) and (13)  $\omega^2 L_c C_c = \beta^2$

(1), (13), and (14)  $\frac{\omega L_c}{R_c} = \frac{\beta}{Q_c}$

Figure 8: 
$$\frac{\bar{c}}{\bar{e}} = \frac{1}{1 - \beta^2 + j \frac{\beta}{Q_c}} \tag{15}$$

Equations (20) and (21)

(19)  $(n+2) \frac{\beta}{\beta^2 - 1} = \frac{\epsilon \beta}{k(1 + \epsilon^2 \beta^2) - 1}$

$$(n+2) \left[ k (1 + \epsilon^2 \beta^2) - 1 \right] = \epsilon (\beta^2 - 1) \quad (19a)$$

$$\beta = 1 \rightarrow (n+2) \left[ k (1 + \epsilon^2) - 1 \right] = 0$$

$$k (1 + \epsilon^2) = 1$$

$$k = \frac{1}{\epsilon^2 + 1} \quad (21)$$

$$1 - k = \frac{\epsilon^2}{\epsilon^2 + 1} \quad (21a)$$

$$(19a) \quad \beta = 0 \rightarrow (n+2) (k - 1) = -\epsilon$$

$$(21a) \quad (n+2) \frac{\epsilon^2}{\epsilon^2 + 1} = \epsilon$$

$$n+2 = \frac{\epsilon^2 + 1}{\epsilon}$$

$$n = \frac{(\epsilon - 1)^2}{\epsilon} \quad (20)$$

Equation (22)

$$(20) \quad n = \frac{(\epsilon - 1)^2}{\epsilon}$$

$$(21) \quad k = \frac{1}{\epsilon^2 + 1}$$

$$(3) \quad \frac{\bar{a}}{\bar{e}} = \frac{n}{n+2} \cdot \frac{-1}{1 - j \frac{\beta}{\beta^2 - 1} (n+2)}$$

$$(11) \quad \frac{\bar{c}}{\bar{e}} = \frac{1}{1 + j \epsilon \beta} - k$$

Substitution of (20) in (3) gives

$$\frac{\bar{a}}{\bar{e}} = \frac{\epsilon (\epsilon - 1)^2}{\epsilon^2 + 1} \cdot \frac{\beta^2 - 1}{\epsilon (1 - \beta^2) + j \beta (\epsilon^2 + 1)} \quad (3a)$$

Substitution of (21) in (11) gives

$$\frac{\bar{c}}{\bar{e}} = \frac{\epsilon}{\epsilon^2 + 1} \cdot \frac{\epsilon (1 - \beta^2) - j \beta (\epsilon^2 + 1)}{\epsilon^2 \beta^2 + 1} \quad (11a)$$

$$(18) \quad \text{tg } \phi = \frac{\bar{a}}{\bar{c}}$$

Substitution of (3a) and (11a) in (18) gives

$$\begin{aligned} \text{tg } \phi &= (\epsilon - 1)^2 \frac{(\beta^2 - 1) (\epsilon^2 \beta^2 + 1)}{\epsilon^2 (1 - \beta^2)^2 + \beta^2 (\epsilon^2 + 1)^2} \\ &= \frac{(\epsilon - 1)^2 (\beta^2 - 1)}{\epsilon^2 + \beta^2} \end{aligned} \quad (22)$$

Equations (24) and (25)

$$(23) \quad \frac{2}{Q} \cdot \frac{\beta}{\beta^2 - 1} = \frac{\epsilon \beta}{k(1 + \epsilon^2 \beta^2) - 1}$$

$$2k + 2k \epsilon^2 \beta^2 - 2 = Q \epsilon \beta^2 - \epsilon Q \quad (23a)$$

$$\beta = 1 \rightarrow 2k + 2k \epsilon^2 - 2 = 0$$

$$k = \frac{1}{\epsilon^2 + 1} \quad (25)$$

$$1 - k = \frac{\epsilon^2}{\epsilon^2 + 1} \quad (25a)$$

$$(23a) \quad \beta = 0 \rightarrow 2k - 2 = -\epsilon Q$$

$$1 - k = \frac{\epsilon Q}{2}$$

$$(25a) \quad \frac{\epsilon^2}{\epsilon^2 + 1} = \frac{\epsilon Q}{2}$$

$$Q = \frac{2 \epsilon}{\epsilon^2 + 1} \quad (24)$$

Equation (26)

$$(8) \quad \frac{\bar{a}}{\bar{e}} = \frac{1}{1 - j \frac{\beta}{\beta^2 - 1} \cdot \frac{2}{Q_a}}$$

$$(11) \quad \frac{\bar{c}}{\bar{e}} = \frac{1}{1 + j \epsilon \beta} - k$$

Substitute (24) in (8):

$$\frac{\bar{a}}{\bar{e}} = \frac{\epsilon (\beta^2 - 1)}{\epsilon (\beta^2 - 1) - j \beta (\epsilon^2 + 1)} \quad (8a)$$

Substitute (25) in (11):

$$\frac{\bar{c}}{\bar{e}} = \frac{\epsilon}{\epsilon^2 + 1} \cdot \frac{\epsilon (1 - \beta^2) - j \beta (\epsilon^2 + 1)}{\epsilon^2 \beta^2 + 1} \quad (11a)$$

Substitute (8a) and (11a) in (18):

$$\text{tg } \phi = \frac{(\epsilon^2 + 1) (\epsilon^2 \beta^2 + 1) (\beta^2 - 1)}{\epsilon^2 (\beta^2 - 1)^2 + \beta^2 (\epsilon^2 + 1)^2}$$

$$= \frac{(\epsilon^2 + 1)(\beta^2 - 1)}{\epsilon^2 + \beta^2} \quad (26)$$

Equation (29)

$$(8) \quad \frac{\bar{a}}{\bar{e}} = \frac{1}{1 - j \frac{\beta}{\beta^2 - 1} \cdot \frac{2}{Q_a}}$$

$$(15) \quad \frac{\bar{c}}{\bar{e}} = \frac{1}{1 - \beta^2 + j \frac{\beta}{Q_c}}$$

$$(18) \rightarrow \text{tg } \phi = \frac{(\beta^2 - 1) \left( 1 - \beta^2 + j \frac{\beta}{Q_c} \right)}{(\beta^2 - 1 - j \beta \frac{2}{Q_a})}$$

with (28)

$$Q_a = 2 Q_c$$

$$\text{tg } \phi = 1 - \beta^2 \quad (29)$$

Equation (34)

Frequency dependent part of (22) and (26):

$$\text{tg } \phi = \frac{\beta^2 - 1}{\beta^2 + \epsilon^2}$$

(32)

$$\beta = 1 + \Delta$$

$$\beta^2 = 1 + 2\Delta + \Delta^2$$

$$\operatorname{tg} \phi = \frac{\Delta^2 + 2\Delta}{1 + 2\Delta + \Delta^2 + \epsilon^2}$$

$$(33) \rightarrow \frac{\Delta^2 + 2\Delta}{1 + 2\Delta + \Delta^2 + \epsilon^2} = - \frac{\Delta^2 - 2\Delta}{1 - 2\Delta + \Delta^2 + \epsilon^2}$$

$$(\Delta + 2)(\epsilon^2 + 1 - 2\Delta + \Delta^2) = (2 - \Delta)(\epsilon^2 + 1 + 2\Delta + \Delta^2)$$

There are two solutions:

$$\Delta = 0 \text{ and } \Delta^2 = 3 - \epsilon^2$$

Taking the last one:

$$\epsilon^2 = 3 - \Delta^2$$

Equation (43)

$$(3) \quad \frac{\bar{a}}{e} = \frac{n}{n+2} \cdot \frac{-1}{1 - j \frac{\beta}{\beta^2 - 1} (n+2)}$$

(32)

$$\beta = 1 + \Delta$$

$$\beta^2 - 1 = \Delta(2 + \Delta)$$

$$\left( \frac{\beta}{\beta^2 - 1} \right)_{\Delta \rightarrow 0} = \frac{1 + \Delta}{\Delta (2 + \Delta)} \longrightarrow \frac{1}{2 \Delta}$$

$$(3) \quad \left( \frac{\bar{a}}{\bar{e}} \right)_{\Delta \rightarrow 0} = \frac{n}{n + 2} \cdot \frac{-1}{1 - j \frac{n + 2}{2 \Delta}}$$

$$= \frac{n}{n + 2} \cdot \frac{-2 j \Delta}{n + 2}$$

$$= - \frac{2 j n \Delta}{(n + 2)^2}$$

$$(42) \quad S_o = \left| \frac{\bar{a}}{\Delta} \right|_{\bar{e}} = 1 \text{ Volt}$$

$$= \frac{2n}{(n + 2)^2} \tag{43}$$

Equation (44)

$$(8) \quad \frac{\bar{a}}{\bar{e}} = \frac{1}{1 - j \frac{\beta}{\beta^2 - 1} \cdot \frac{2}{Q_a}}$$

$$\beta \rightarrow 1 \text{ or } \Delta \rightarrow 0 \text{ gives } \frac{\beta}{\beta^2 - 1} \longrightarrow \frac{1}{2 \Delta}$$

$$\left( \begin{array}{c} - \\ a \\ - \\ e \end{array} \right) \Delta \rightarrow 0 = \frac{1}{1 - \frac{j}{\Delta Q_a}}$$

$$= j \Delta Q_a$$

$$(42) \quad \rightarrow S_o = Q_a$$

$$(44)$$

## D I S T R I B U T I O N   L I S T

Minister of Defense Brussels, Belgium	10 copies	Commander in Chief Western Atlantic Area (CINCWESTLANT) Norfolk 11, Virginia	1 copy
Minister of National Defense Department of National Defense Ottawa, Canada	10 copies	Commander in Chief Eastern Atlantic Area (CINCEASTLANT) Eastbury Park, Northwood Middlesex, England	1 copy
Chief of Defense, Denmark Kastellet Copenhagen Ø, Denmark	10 copies	Maritime Air Commander Eastern Atlantic Area (COMAIREASTLANT) R. A. F. Northwood Middlesex, England	1 copy
Minister of National Defense Division Transmissions-Ecoute-Radar 51 Latour Maubourg Paris 7 <sup>e</sup> , France	10 copies	Commander Submarine Force Eastern Atlantic (COMSUBEASTLANT) Fort Blockhouse Gosport, Hants, England	1 copy
Minister of Defense Federal Republic of Germany Bonn, Germany	10 copies	Commander, Canadian Atlantic (COMCANLANT) H. M. C. Dockyard Halifax, Nova Scotia	1 copy
Minister of Defense Athens, Greece	10 copies	Commander Ocean Sub-Area (COMOCEANLANT) Norfolk 11, Virginia	1 copy
Ministry of National Defense Navy General Staff Rome, Italy	10 copies	Supreme Allied Commander Europe (SACEUR) Paris, France	7 copies
Minister of National Defense Plein 4, The Hague, Netherlands	10 copies	SHAPE Air Defence Technical Center P. O. Box 174 Stadhouders Plantsoen 15 The Hague, Netherlands	1 copy
Minister of National Defense Storgaten 33, Oslo, Norway	10 copies	Allied Commander in Chief Channel (CINCCHAN) Fort Southwick, Fareham Hampshire, England	1 copy
Minister of National Defense, Portugal Care Portuguese Military Attaché 3 Rue Noisiel Paris, France	10 copies	Commander Allied Maritime Air Force Channel (COMAIRCHAN) Northwood, England	1 copy
Minister of National Defense Ankara, Turkey	10 copies	Commander in Chief Allied Forces Mediterranean (CINCAF MED) Malta, G. C.	1 copy
Minister of Defense London, England	18 copies	Commander South East Mediterranean (COMEDSOUEAST) Malta, G. C.	1 copy
Supreme Allied Commander Atlantic (SACLANT) Norfolk 11, Virginia	5 copies		
SACLANT Representative in Europe (SACLANTREPEUR) Place du Marechal de Lattre de Tassigny Paris 16 <sup>e</sup> , France	1 copy		

Commander Central Mediterranean (COMEDCENT) Naples, Italy	1 copy	NLR United Kingdom British Defence Staffs, Washington 3100 Massachusetts Avenue, N. W. Washington, D. C.	1 copy
Commander Submarine Mediterranean (COMSUBMED) Malta, G. C.	1 copy	NLR United States SACLANT Norfolk 11, Virginia	40 copies
<u>National Liaison Representatives</u>		<u>Scientific Committee of National Representatives</u>	
NLR Belgium Belgian Military Mission 3330 Garfield Street, N. W. Washington, D. C.	1 copy	Dr. J. E. Keyston Defense Research Board Department of National Defense Ottawa, Canada	1 copy
NLR Canada Canadian Joint Staff 2450 Massachusetts Avenue, N. W. Washington, D. C.	1 copy	G. Meunier Ingenieur en Chef des Genie Maritime Services Technique des Constructions et Armes Navales 8 Boulevard Victor Paris 15 <sup>e</sup> , France	1 copy
NLR Denmark Danish Military Mission 3200 Whitehaven Street, N. W. Washington, D. C.	1 copy	Dr. E. Schulze Bundesministerium der Verteidigung ABT H ROMAN 2/3 Bonn, Germany	1 copy
NLR France French Military Mission 1759 "R" Street, N. W. Washington, D. C.	1 copy	Commander A. Pettas Ministry of National Defense Athens, Greece	1 copy
NLR Germany German Military Mission 3215 Cathedral Avenue, N. W. Washington, D. C.	1 copy	Professor Dr. Maurizio Federici c/o MARICOMITARMI Ministero della Marina Rome, Italy	1 copy
NLR Greece Greek Military Mission 2228 Massachusetts Avenue, N. W. Washington, D. C.	1 copy	Dr. M. W. Van Batenburg Fysisch Laboratorium RVO-TNO Waalsdorpvlaakte The Hague, Netherlands	1 copy
NLR Italy Italian Military Mission 3221 Garfield Street, N. W. Washington, D. C.	1 copy	Mr. A. W. Ross Department of Physical Research Admiralty, Whitehall London S. W. 1, England	1 copy
NLR Netherlands Netherlands Joint Staff Mission 1470 Euclid Street, N. W. Washington, D. C.	1 copy	Dr. J. E. Henderson Department of Physics University of Washington Seattle 5, Washington	1 copy
NLR Norway Norwegian Military Mission 2720 34th Street, N. W. Washington, D. C.	1 copy	.....	
NLR Portugal Portuguese Military Mission 2310 Tracy Place, N. W. Washington, D. C.	1 copy	Standing Group, NATO (SGN) Room 2C256, The Pentagon Washington 25, D. C.	3 copies
NLR Turkey Turkish Joint Staff Mission 2125 LeRoy Place, N. W. Washington, D. C.	1 copy	Standing Group Representative (SGREP) Place du Marechal de Lattre de Tassigny Paris 16 <sup>e</sup> , France	5 copies